Appendix A

Analysis of Data from Davidson et. al. (2004) Paper

The Data

The raw data were provided by the authors in a personal communication to Dr. Leo Korn (DSRT/NJDEP) in the form of an Excel spreadsheet. The study is described in Davidson et. al. (2004). All of the mice included in the provided data were exposed to UV. The Excel data were converted to a SAS data set. A printout of the data is attached (see Table A.2). All tumors were tested for malignancy in the two lower dose groups (0 ppm and 0.5 ppm). In the higher dose groups (2.5 ppm and 5.0 ppm) a random sample from all tumors was tested for malignancy. The number of malignant tumors will always be less than or equal to the number of tumors diagnosed.

Data Analysis Strategies

The possible outcome measures of interest are:

1. Number of mice with tumors
2. Number of tumors per mouse.
3. Number of mice with malignancies.
4. Number of malignancies per mouse.
5. Proportions of malignant tumors per mouse.

It is of interest whether there is a relationship between magnitude of dose and these five outcomes.

Table A.1. Davidson Data

Davidson Data

Mouse ID	Chromium Dose (ppm)	Number of Tumors > 2mm	Number of Tumors Diagnosed	Number of Malignant Tumors
16	0.0	0	0	0
17	0.0	2	2	1
18	0.0	0	0	0
19	0.0	0	0	0
20	0.0	1	1	1
21	0.0	1	1	0
22	0.0	4	4	2
23	0.0	0	0	0
24	0.0	1	1	1
25	0.0	1	1	0
26	0.0	0	0	0
27	0.0	0	0	0
28	0.0	0	0	0
29	0.0	1	1	1
3	0.0	0	0	0
31	0.5	1	1	1
33	0.5	1	1	0
35	0.5	0	0	0
36	0.5	3	3	1
37	0.5	0	0	0
38	0.5	0	0	0
39	0.5	4	4	2
41	0.5	3	3	2
42	0.5	0	0	0
43	0.5	2	2	1
44	0.5	0	0	0
46	2.5	2	2	1
47	2.5	0	0	0
48	2.5	0	.	.
49	2.5	2	.	.
50	2.5	2	2	2
51	2.5	5	3	1
52	2.5	1	.	.
53	2.5	0	.	.
54	2.5	1	.	.
55	2.5	0	.	.

Davidson Data

Mouse ID	Chromium Dose (ppm)	Number of Tumors > 2mm	Number of Tumors Diagnosed	Number of Malignant Tumors
56	2.5	2	.	.
57	2.5	2	.	.
58	2.5	0	.	.
59	2.5	3	.	.
60	2.5	0	0	0
61	2.5	10	.	.
62	2.5	5	.	.
63	2.5	1	.	.
64	2.5	11	.	.
106	5.0	5	.	.
107	5.0	2	.	.
108	5.0	5	.	.
109	5.0	9	4	2
110	5.0	4	.	.
111	5.0	2	.	.
112	5.0	4	3	2
113	5.0	2	.	.
114	5.0	0	.	.
115	5.0	0	.	.
116	5.0	4	.	.
117	5.0	9	.	.
118	5.0	4	3	3
119	5.0	0	.	.
120	5.0	10	2	1
121	5.0	10	.	.
122	5.0	17	.	.
123	5.0	0	.	.
124	5.0	3	3	3

Number of Mice with Tumors

Table A.2 presents the proportion of mice with tumors in each dose group.

Table A.2: Proportion of Mice with Tumors in Each Group

Dose (ppm)	Number of Mice	Proportion of Mice with Tumors
0	15	0.4666667
0.5	11	0.5454545
2.5	19	0.6842105
5	19	0.7894737

There appears to be a relationship between dose and proportion of mice with tumors. The statistical significance of this relationship can be ascertained by the Jonckheere-Terpstra test. This is a non-parametric test for trend. The two-sided p-value for this test is .0002. The observed trend is highly significant.

Another way to look at the relationship is through a logistic regression model, which predicts the probability of a mouse having at least one tumor as a linear function of dose. The estimated dose parameter in this model is 0.2849 (p=0.0450). There is a significant positive relationship between dose and probability of tumor. The odds ratio for a 1 ppm increase in dose is 1.33 with a 95% confidence interval of (1.006, 1.757).

Number of Tumors per Mouse

Table A.3 presents the average number of tumors per mouse in each dose group.

Table A.3: Average Number of Tumors>2mm in Each Group

Dose (ppm)	N	Average Number of Tumors	Std Dev	Minimum	Maximum
0	15	0.7333333	1.0997835	0	4
0.5	11	1.2727273	1.4893562	0	4
2.5	19	2.4736842	3.2209112	0	11
5	19	4.7368421	4.4701741	0	17

There appears to be a relationship between dose and the average number of tumors. The statistical significance of this relationship can be ascertained by a Poisson Regression model, which predicts the expected number of tumors, by a function of dose. The estimated parameter for dose is 0.3199 ($p<0.0001$) so the observed trend is highly significant.

Graphically, the relationship can be illustrated in Figure 1. In the plot, the stars represent one or more data points and the diamonds represent the average count in each dose group. Line segments connect the average counts. The increasing trend in the average counts can be clearly seen.

Number of Mice with Malignancies

The analysis of malignancies is more complicated due to the random sampling of tumors at higher doses. Since selection was randomized with respect to tumors rather than with respect to mice, mice with large numbers of tumors would be more likely to be sampled than mice with only a few tumors. If there is an association between the number of tumors and the probability of malignancy then the analysis might be biased. On the other hand, an examination of the data in the two highest dose groups does not show a gross over-sampling of mice with many tumors. Table A.4 breaks down the number of samples taken from mice with the specified number of tumors. From Table A.4 one can see that tumors were sampled from mice with 2 tumors and 5 tumors in dose group 2.5 and from mice with 3,4,9 and 10 tumors in dose group 5. Mice with 10 tumors and 11 tumors were not sampled in dose group 2.5. A mouse with 17 tumors and one of the mice with 10 tumors were not sampled in dose group 5

Table A.4: Number of Samples taken from Mice with Specified Number of Tumors

Dose	# Total tumors per mouse >2mm	# Tumors per mouse diagnosed for malignancy	Number of mice
0	1	1	5
0	2	2	1
0	4	4	1
0.5	1	1	2
0.5	2	2	1
0.5	3	3	2
0.5	4	4	1
2.5	2	2	2
2.5	5	3	1
5	3	3	1
5	4	3	2
5	9	4	1

5	10	2	1

There are several ways to count proportions. Since some mice have no tumors, they may be counted as mice with no malignancy. If the mice with no tumors are included in the counting, the proportions of mice with malignancies in each dose group are shown in Table A.5.

Table A.5: the proportions of mice (with malignancies, counting mice with no tumors)

Dose	N	Proportion of Mice with Malignancy
0	15	0.3333333
0.5	11	0.4545455
2.5	19	0.3333333
5	19	0.5555556

Table A.5 does not show a well-defined trend. A logistic regression model has a non significant parameter estimate for dose, (0.13, $p<0.42$). There is no evidence of a dose response relationship when looking at the data in this way.

If mice with no tumors were not counted as having zero malignancies, this could be considered an analysis conditioned on mice with tumors. In this case the proportions of mice with malignancies are given in Table A.6.

Table A.6: The proportions of mice with malignancies (omitting mice with no tumors)

Dose	N	Proportion of Mice with Malignancy
0	7	0.7142857
0.5	6	0.8333333
2.5	3	1.0000000
5	5	1.0000000

While there does appear to be a defined trend in the observed proportions, the sample sizes are very small and the logistic regression is not significant (dose parameter estimate=1.7, $p<0.42$).

Number of Malignancies per Mouse

Interpreting the average number of malignancies per mouse is perilous, since it will be dependent to some extent on the number of tumors per mouse and the number of tumors sampled per mouse. Even if a dose-response is clearly evident, it is not obvious what it means. Table A.7 presents the average number of malignancies per mouse in each dose group, including mice with zero tumors.

Table A.7: Average number of malignancies per mouse

Dose	N	Average # Malignancies	Minimum	Maximum
0	15	0.4000000	0	2.
0.5	11	0.6363636	0	2
2.5	19	0.8000000	0	2
5	19	2.2000000	1	3

This Table A.7 shows a well-defined trend. A Poisson regression model indicates that the dose parameter is significant (0.3133, p<. 001).

Proportions of Malignant Tumors per Mouse

The proportion of malignant tumors per mouse is defined as the number of malignancies divided by the number of tumors tested. Those mice with no tumors may be counted as either undefined or as zero. Tables A.8 and A.9 present these results.

Table A.8: Mean Proportion of Malignancies with Zero Tumors Counted as Zero Proportion

Dose	N	Mean Proportion
0	15	0.2666667
0.5	11	0.2727273
2.5	9	0.2037037
5	19	0.4074074

Table A.9: Mean Proportion of Malignancies with Zero Tumors Not Counted

Dose	N	Mean Proportion
0	7	0.5714286
0.5	6	0.5000000
2.5	3	0.6111111
5	5	0.7333333

In both tables, the trends are not well defined. Note that the sample sizes are quite small in table 8. Tests of significance were not performed on the data of Tables A.8 and A.9.

Conclusions

There is a significant relationship between dose and counts of total tumors, dose and proportion of mice with tumors, and dose and malignancy counts. The interpretation of malignancy counts is difficult due to the sampling scheme and the relationship between number of total tumors and number of malignancies.

References

1. Davidson, T., Kluz, T., Burns, F., Rossman, T., Zhang, Q., Uddin, A., Nadas, A., Costa, *M. (2004). Exposure to chromium (VI) in the drinking water increases susceptibility to UV-induced skin tumors in hairless mice.* Toxicology and Applied Pharmacology (in press).

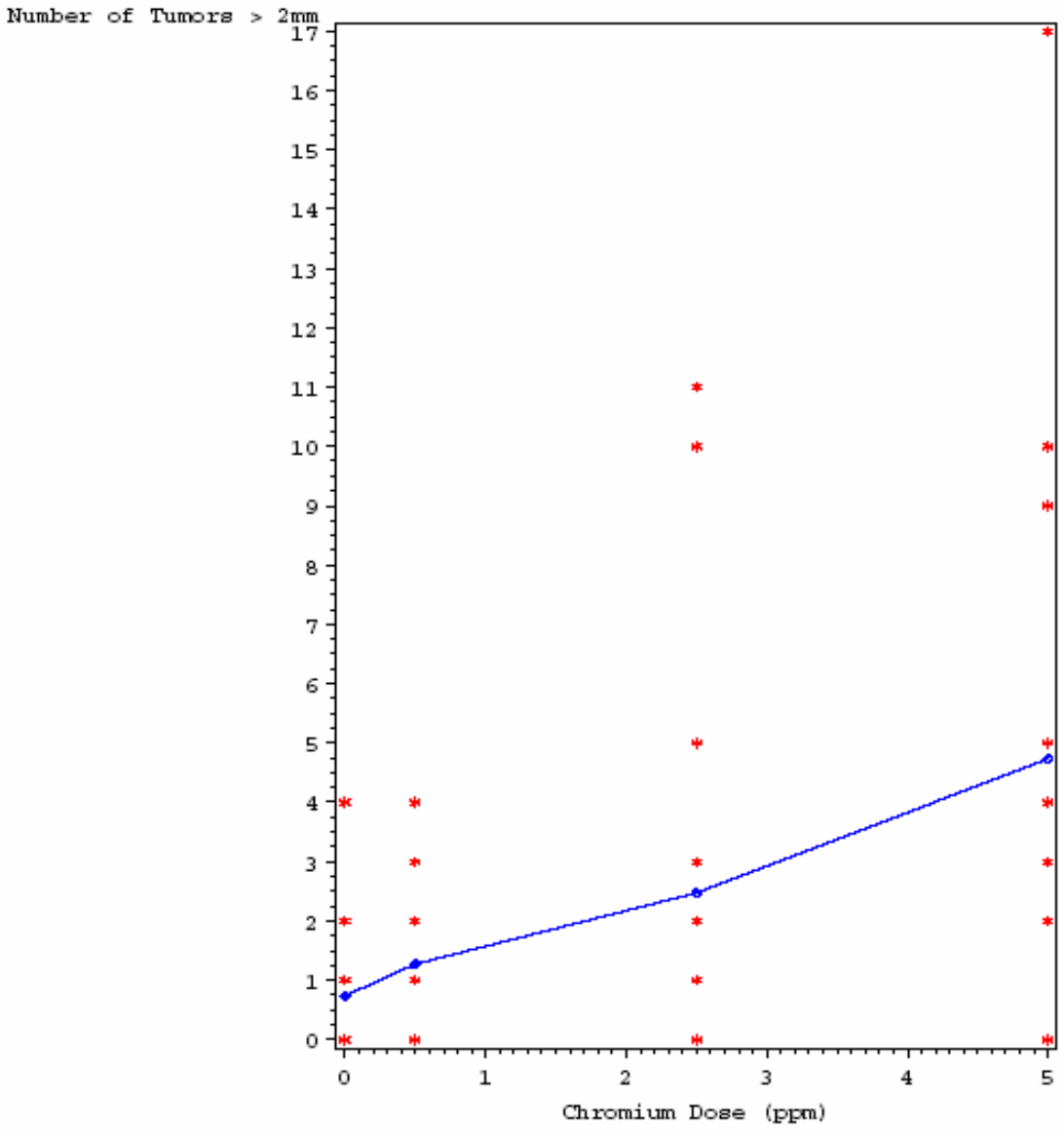

Figure A.1: Number of Tumors Greater than 2mm

Appendix B

Background Information on the Physics and Biology of UV Radiation with Reference to the Exposures in Davidson et al. (2004)

DEFINITIONS AND CONVERSION FACTORS

Action Spectrum	An action spectrum is a range of wavelengths in which biological effectiveness can be defined.
Biological Effectiveness -	The biological effectiveness is a measure of the effectiveness of radiation at different wavelengths (within a defined range or action spectrum) in carrying out a specific reproducible photobiological process.
Irradiance -	The unit of radiant power per unit area (Watt/cm^2) is the irradiance.
MED -	Minimal erythema dose.
Radiant Exposure (Dose) -	The unit of radiant energy per unit area (joules/ cm^2) is the radiant exposure.
Relative Biological Effectiveness -	The relative biological effectiveness is an experimentally determined ratio of an absorbed dose of a reference radiation required to produce an identical biological effect in a particular organism or tissue.

Radiant Energy Units

	erg	joule	W sec	µW sec
erg=	1	10^{-7}	10^{-7}	0.1
joule=	10^7	1	1	10^6
W sec=	10^7	1	1	10^6
µW sec=	10	10^{-6}	10^{-6}	1

Radiant Exposure (exposure dose) Units

	Erg/cm^2	joule/cm^2	W sec/cm^2	µW sec/cm^2
erg/$cm^{2=}$	1	10^{-7}	10^{-7}	0.1
joule/cm^2=	10^7	1	1	10^6
W sec/cm^2=	10^7	1	1	10^6
µW sec/cm^2	10	10^{-6}	10^{-6}	1

Irradiance (exposure dose rate) Units

	Erg/$cm^{2.}$ sec	joule/$cm^{2.}$ sec	W/cm· sec^2	µW/$cm^{2.}$ sec
erg/$cm^{2.}$ $sec^{=}$	1	10^{-7}	10^{-7}	0.1
joule/$cm^{2.}$ sec =	10^7	1	1	10^6

W /cm^2 =	10^7	1	1	10^6
$\mu W/cm^2$=	10	10^{-6}	10^{-6}	1

Ultraviolet radiation is at shorter wavelengths than the visible spectrum (400 to 700nm). In physics applications UV is divided into three components (NASA, 2004):

UVA - 315 to 400 nm (Long wave)
UVB - 280 to 315 nm (GE does not make these)
UVC - less than 280 nm

Environmental photobiologists normally define wavelength regions slightly differently as:
UVA - 320 to 400 nm
UVB - 290 to 320 nm
UVC 200 to 290 nm (Diffey, 1991)

The division between UVB and UVC is chosen at 290 nm because UV radiation (UVR) at shorter wavelengths is unlikely to be present in terrestrial sunlight except at high altitudes (Henderson 1977, as cited by Diffey, 1991).

Physics of Ultraviolet light:

Sunlight

Most of the light that hits the earth comes from our sun which emits radiation with wavelengths as short as 100 nanometers (nm = millimicron = mμ). Oxygen in the upper atmosphere absorbs most of the radiation shorter than ~ 200 nm. This process produces ozone, which absorbs strongly with a maximum at 253 nm, but a weak tail extends to approximately 330 nm. This edge of the ozone absorption band determines the cut-off of ultraviolet (UV) that reaches the earth. Except at high altitude, very little light < 295 nm reaches earth.

Light is scattered by the atmosphere and by particulates, which can both scatter and absorb radiation (light). Light interaction with air molecules causes Raleigh scattering which is a function of wavelength: shorter wavelengths, such as UV being scattered more. As much as two thirds of the UV at 310 nm is scattered.

Ozone (O3) is formed by dissociation of oxygen by short wavelength UVR (lambda <242 nm) at altitudes of 25 to 100 km. Absorption of UVR at wavelengths up to 320 nm converts the O3 back to O2 and O (Chapman 1930, as cited by Diffey, 1991). Dissociation of O3 is responsible for preventing wavelengths less than about 290 nm from reaching the Earth's surface.

The spectral irradiance of UVR on the Earth's surface is modified by temporal, geographical, and meteorological factors such that the UV spectral irradiance falls by a factor of two or three as the wavelengths decrease from 400 to 320 nm at solar altitudes higher than 20 degrees. They drop rapidly by three orders of magnitude or more from 320 to 290 nm by the absorption of stratospheric ozone (Diffey, 1991).

The energy in about a 3-minute sunlight exposure (UVA, primarily 365 nm) would be:

Dosage Energy = UV Intensity X Time
= 2.5 mW/cm2 X 200 sec
= 500 mJ/cm2
Where:

mW = milliwatts
mJ = millijoules

UV Lamps

Hill and Hill (2000) reported the following spectral distributions for the Westinghouse lamp used by Davidson et al. (2004).

Westinghouse polychromatic FS20: 0.0065 % UVC, 42.3% UVB, 37.3 % UVA, and 23.8 % visible.

The FS-20 lamp emits an energy spectrum with a high influence in the 280 - 360 nm UVB region peaking at 313 nm (as cited in Peus et al., 2000 and Mitchell et al., 2002).

Davidson et al. (2004) reported that less than 1% of the UV light from the FS-20 lamps was in the UVC range, while 85% was in the UVB spectral range (320 - 400 nm) and the visible spectrum. Hill and Hill (2000) independently reported the FS-20 bulb emitting 0.0065% in the UVC spectral.

General Electric Lighting Company via e-mail. Technical specialist Donna L. Quesenberry (GE Consumer & Industrial), provided the following information:

The only lamps GE makes in the UV range are germicidal (UVC 100-280 nm) and the blacklight (white glass-blue light)/blacklight blue (blue glass-blue light) (315-400nm, UVA). GE does not make any UVB lamps which are sometimes used for medical purposes or tanning beds.

Some wavelengths (180-220) produce ozone, some (220-300) are bactericidal, some (280-320) erythemal (redden human skin), others (320-400) cause secondary luminance (blacklight).

Spectral Distribution curves are available in the GE Lighting Application Bulletin which is available in e-doc (keyword blacklight or UVA).

Two faxed pages contained SPB UV and BL/BLB UV Maintenance curves (Percent UV emitted versus Lamp Life in hours of usage) and BLB and BL Spectral Power curves comparing Irradiance expressed as W/cm2/nm versus Wavelength in nm. These curves for the BL lamp showed maximal peaks at ~375 (range 350 to 400), and visible light peaks at ~410 (very minimal), a middle value peak at ~440, and a smaller peak at 550 nm.

Biology of Ultraviolet light:

Diffey (1991) discusses molecular and cellular ultraviolet photobiology, absorption characteristics of important biomolecules, action spectra, photoproducts, inactivation of microorganisms, and repair mechanisms. Observable biological effects in man due to UVR are limited to the skin and eyes because of the low penetrating properties of UVR in human tissues. Penetration is less than 1 mm in skin (Bruls et al., 1984; as cited by Diffey, 1991) and UVR is absorbed by ocular tissues, mainly the cornea and the lens, before reaching the retina.

Acute reactions of UVR on the skin are sunburn, tanning, and vitamin D production. Photo-aging and skin cancer are considered chronic reactions produced by prolonged or repeated UVR exposures.

Sunburn, or erythema, is an acute injury following excessive exposure to sunlight. Redness of the skin results from an increased blood content of the skin by dilatation of the superficial blood vessels in the dermis, mainly the subpapillary venules. Half an hour of midday summer sunshine in the UK on the unacclimatized skin of Caucasian subjects is normally sufficient to elicit a subsequent mild reddening of the skin. Erythema reaches a maximum about 8 to 12 hours later and fades within 1 to 2 days (Olson et al., 1996; Farr et al., 1988; as cited by Diffey, 1991). Repeated exposures to sunlight for longer periods progressively shortens the time before appearance of erythema, lengthens the persistence, and increases its intensity. High exposures may result in edema, pain, blistering, and, after a few days, peeling.

The minimal erythema dose or MED at a given wavelength in a group of fair-skinned individuals is distributed lognormally. In 254 normal subjects in North East England the MED at 300 nm was determined to be 34 mJ/cm^2 with a 95% confidence interval of 14-84 mJ /cm^2 (Diffey, 1991). Above 300 nm the effectiveness drops rapidly, falling to an efficiency at 320 nm of about 1% of that at 300 nm. The erythema action spectrum up to 400 nm has been determined, although the rate of change of effectiveness is much less from 330 to 400 nm, than from 300 to 330 nm.) Figure B.1 shows an action spectrum accepted by the Commission Internationale de l'Eclairage (CIE) and the International Electrotechnical Committee (IEC) and has been shown to predict accurately the erythemal effectiveness of several polychromatic light sources differing greatly in spectral composition (Urbach 1987, as cited by Diffey, 1991). Learn et. al., (1993) reported that for an equal amount of energy delivered, radiation from the unfiltered lamps was more potent in causing the erythemal response than filtered lamps that removed the UVC spectral component of that lamp. Specifically, on a power versus response basis 3.2 % of the power for UVC was responsible for an average of 13.9 % (11.1 and 16.7%) of the erythemal response.

Although UVA is much less erythmogenic than UVB, broadly speaking by a factor of 1000, the much higher UVA present in sunlight means in summertime UVA radiation contributes about 15 to 20% to the sunburn reaction.

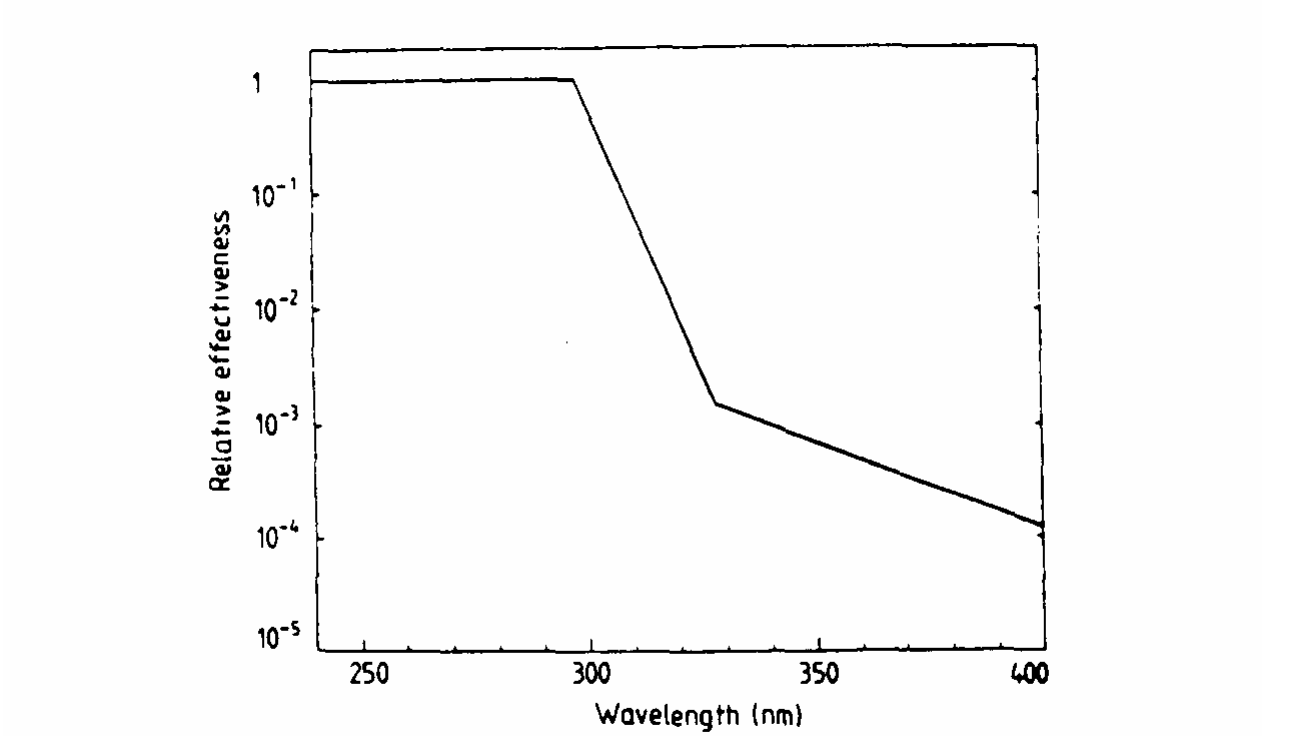

Figure B.1: The CIE Reference Erythema Action Spectrum [McKinlay and Diffey (1987)

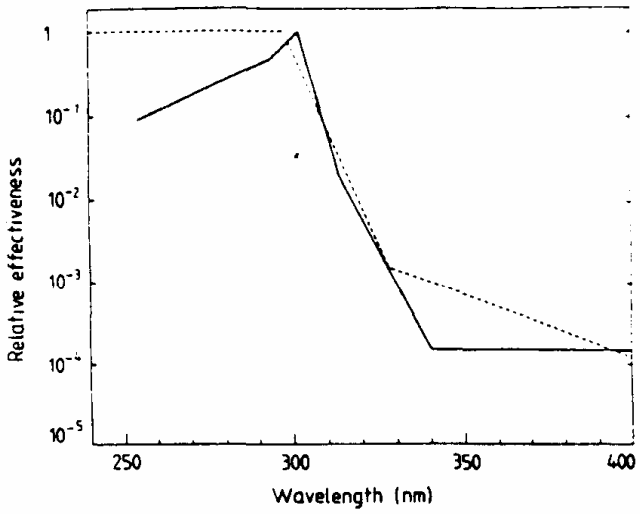

Figure B.2: The absorption spectrum of nucleic acids and the action spectrum for the inactivation of *E. coli*. cells [reproduced from Harm (1980)].

Figure B.2 compares the CIE Reference Erythema Action Spectrum to the action spectrum for UV photocarcinogenesis. Note that the action spectra for photocarcinogenesis is at a maximum at about 302 nm and drops by a factor of 10 at approximately 254 nm, whereas, the erythema action spectra is maximal from about 297 to below 254 nm. At wavelengths greater than 290 nm there is reasonable agreement between the curves. Thus, while UVC is generally more effective than UVB in producing erythema, it is much less effective in production of tumors. An explanation for this difference is suggested by Figure B.3. It appears that while UVC radiation is readily absorbed by nucleic acids, the extent of damage due to the large amount of energy transfer produces irreversible damage leading to cell death rather than to viable cells with inheritable mutations. Thus, the curves for nucleic acid absorption and cell inactivation closely

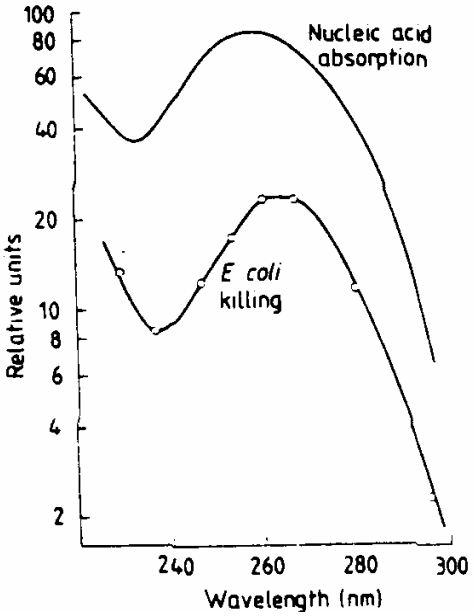

Figure B.3: The absorption spectrum of nucleic acids and the action spectrum for the inactivation of *E. coli cells (reproduced from Harm (1980))*

parallel each other.

With respect to the UV exposures in the Davidson et al. (2004) study, the UVC radiation appears to have contributed considerably less than 1% to the total UVR output of the Westinghouse lamps and noe of the ouitput of the GE lamps. Thus, some minor fraction of the total UV radiation was of a UVC with wavelength that is not available in the natural sunlight reaching the ground surface every day in New Jersey. However, the action spectra of UVC at these wavelengths is only about 1/10 the effectiveness for causing photocarcinogenesis as for causing erythema. Therefore, given that the Westignhouse lamps produced UVR containing less than 1% UVC, and that UVC is less than 10% as effective as UVB in the prodcution of skin tumors, , it does not seem likely that the UVC radiation received by the mice in this study made a significant contribution to the observed tumor production compared to the other wavelengths of UV radiation they received

References:

Davidson, T., Kluz, T., Burns, F., Rossman, T., Zhang, Q., Uddin, A., Nadas, A., and M. Costa. 2004. Exposure to Chromium (VI) in the Drinking Water Increases Susceptibility to UV-Induced Skin Tumors in Hairless Mice. Tox. Appl. Pharmacol. 196(3):431-437.

Diffey, B. L. 1991. Solar Ultraviolet Radiation Effects on Biological Systems. Review in Physics in Medicine and Biology 36(3):299-328.

Henderson, S. T. 1977. Daylight and its Spectrum (Bristol: Adam Hilger) p.33.

Hill, Helene Z. and George J. Hill. 2000. UVA, Pheomelanin and the Carcinogenesis of Melanoma. Pigment Cell Res. 13 (Suppl. 8): 140-144.

Learn, D. B., Beard, J., and S. J. Moloney. 1993. The Ultraviolet C Energy Emitted from FS Lamps Contributes Significantly to the Induction of Human Erythema and Murine Ear Edema. Photodermatol. Photoimmunol. Photomed. 9:147-153.

McKinlay, a. F., and B. L. Diffey. 1987. A Reference Action Spectrum for Ultra-Violet-Induced Erythema in Human Skin. In: Passchier, W. F. and B. F. M. Bosnjakovic, (eds.). Human Exposure to Ultraviolet Radiation: Risks and Regulations. Amsterdam: Elsevier, 1987:83-96.

Mitchell, D. L., Meador, J., Paniker, L., Gasparutto, D., Jeffrey, W. H., and J. Cadet. 2002. Development and Application of a Novel Immunoassay for Measuring Oxidative DNA Damage in the Environment. Photochem. Photobiol. 75(3):257-265.

NASA. 2004. Datad Product: Erythemal UV Exposure. National Aeronautics and Space Administration. Goddard Space Flight Center. Revised July 20, 2004. Http://toms.gsfc.nasa.gov/ery_uv/euv.html.

Peus, D., Vasa, R. A., Meves, A., Beyerie A., and M. R. Pittelkow. 2000. UVB-Induced Epidermal Growth Factor Receptor Phosphorylation is Critical for Downstream Signaling and Keratinocyte Survival. Photochem. Photobiol. 72(1):135-140.

Urbach, F. 1982. Photocarcinogenesis. The Science of Photomedicine. Ed. J. D. Regan and J. A. Parrish (New York, Plenum) pp. 261-292.

Appendix C

Benchmark Dose Calculations for Nethercott et al. (1994)

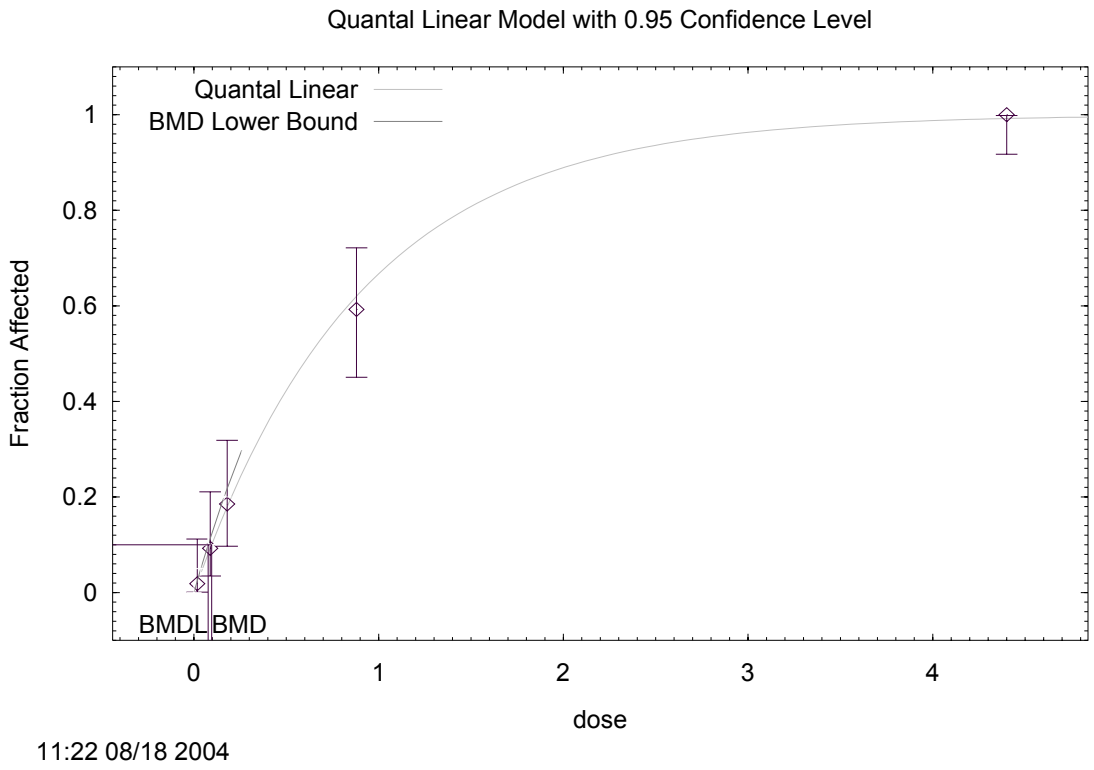

```
================================================================================
        Quantal Linear Model Revision: 2.2 Date: 2000/03/17 22:27:16
        Input Data File: U:\CR WORKGROUP\NETHERCOTT.(d)
        Gnuplot Plotting File:  U:\CR WORKGROUP\NETHERCOTT.plt
                                                    Wed Aug 18 11:22:36 2004
================================================================================

BMDS MODEL RUN
~~~~~~~~~~~~~~~~~~~~~~~~~~~~~~~~~~~~~~~~~~~~~~~~~~~~~~~~~~~~~~~~~~~~~~~~~~~~~~~~

  The form of the probability function is:

  P[response] = background + (1-background)*[1-EXP(-slope*dose)]

  Dependent variable = COLUMN3
  Independent variable = COLUMN1

  Total number of observations = 5
  Total number of records with missing values = 0
  Maximum number of iterations = 250
  Relative Function Convergence has been set to: 1e-008
  Parameter Convergence has been set to: 1e-008

            Default Initial (and Specified) Parameter Values
              Background =         0.5
                 Slope =     0.910758
                 Power =            1   Specified

       Asymptotic Correlation Matrix of Parameter Estimates

       ( *** The model parameter(s)  -Background    -Power
            have been estimated at a boundary point, or have been specified by the user,
            and do not appear in the correlation matrix )

             Slope

  Slope          1

                  Parameter Estimates

    Variable        Estimate        Std. Err.
  Background               0              NA
     Slope         1.10098         0.147508

NA - Indicates that this parameter has hit a bound
    implied by some inequality constraint and thus
    has no standard error.

                Analysis of Deviance Table

     Model      Log(likelihood)  Deviance  Test DF     P-value
   Full model        -84.012
  Fitted model       -84.5343      1.04465     4          0.903
```

Reduced model -179.001 189.977 4 <.0001

AIC: 171.069

Goodness of Fit

Dose	Est._Prob.	Expected	Scaled Observed	Size	Residual
0.0180	0.0196	1.060	1	54	-0.05849
0.0880	0.0923	4.986	5	54	0.006389
0.1800	0.1798	9.708	10	54	0.1035
0.8800	0.6205	33.506	32	54	-0.4224
4.4000	0.9921	53.575	54	54	0.6546

Chi-square = 0.62 DF = 4 P-value = 0.9607

Benchmark Dose Computation

Specified effect = 0.1

Risk Type = Added risk

Confidence level = 0.95

BMD = 0.0956969

BMDL = 0.0770345